

Structures and magic numbers of group-IV microclusters calculated by use of an anisotropic model potential

S. Saito

*Fundamental Research Laboratories, NEC Corporation, Miyazaki, Miyamae-ku, Kawasaki, Kanagawa 213, Japan
and Institute for Solid State Physics, University of Tokyo, Roppongi, Minato-ku, Tokyo 106, Japan*

S. Ohnishi

Fundamental Research Laboratories, NEC Corporation, Miyazaki, Miyamae-ku, Kawasaki, Kanagawa 213, Japan

S. Sugano

Institute for Solid State Physics, University of Tokyo, Roppongi, Minato-ku, Tokyo 106, Japan

(Received 13 December 1985)

A new nonspherical symmetrized potential model for the study of the cohesive properties of covalent systems is presented. The model suitable for microclusters of the sp^3 atoms is applied to determine the stable structures of group-IV microclusters of 2 to 20 atoms. The resulting structures are classified into two groups: crystalline and amorphous types. The crystalline-type structure has six-membered rings and the amorphous-type structure four- and five-membered rings. The pair distribution functions of the crystalline and the amorphous types correspond to the radial distribution function of the crystalline and amorphous germanium, respectively. From the binding energies per atom, magic numbers of the crystalline-type group are found to be 6, 10, 14, and 18, while those of amorphous-type group are 5, 10, 12, 16, 18, and 20.

I. INTRODUCTION

Recent experiments of time-of-flight mass spectra of microclusters have revealed the presence of magic numbers of the cluster size.¹⁻⁵ It is of great interest to understand the origin of the magic numbers from the analysis of the binding properties of microclusters.

Stable structures of model clusters such as those composed of atoms interacting by a two-body central force, for example, the Lennard-Jones force, have been well studied.⁶ The calculated structures and binding energies have been applied successfully for rare-gas clusters. However, covalent clusters have scarcely been studied in this way because of the complicated nature of covalent bonds.

In this paper, we report a new model-potential study of the covalent microclusters, which are composed of the sp^3 -hybridized atoms. In our model, each atom has four attractive centers which form a regular tetrahedron. Our potential is so constructed that the interaction energy depends upon the relative orientation of the anisotropy axes of two atoms. Our potential is, however, unable to take into account a deviation from the sp^3 bonding which may be caused, for instance, by the interaction between the dangling bonds. Hence, our model is expected to express the properties of the silicon and germanium clusters rather than carbon clusters, which can have sp^2 - and sp -hybridization characters as well as sp^3 . It will be discussed that the model potential is useful in finding the stable structure of the first approximation.

To find the stable structure, we minimize the total energy by rotating and translating atoms according to quasi-Newton method. The calculated stable structures being

found tend to have four-, five-, and six-membered rings. We have classified them into two types, according to a characteristic feature of the pair distribution functions, which may be compared with the radial distribution functions of a crystalline and an amorphous germanium.⁷

The magic numbers of our model clusters have been derived from the plot of the binding energy per atom against the number of atoms. The calculated magic numbers resemble those of Si_n^+ and Ge_n^+ clusters determined experimentally.^{4,5}

II. MODEL POTENTIAL

To express the tetrahedral-coordination property of the covalent interaction between sp^3 -hybridized atoms, we introduce the following model system. In our model, each atom is not a material point, but has a certain structure. The four "attractive centers," which constitute a regular tetrahedron, are located around each atom (Fig. 1). The attractive center of one atom tends to attract other atoms. This tendency, combined with short-range repulsive force, is not, however, a sufficient condition for atoms to have tetrahedral coordination. It is desirable that when the i th atom sits on one of the attractive centers of the j th atom, the j th atom also sits on one of the attractive centers of the i th atom. This restriction excludes the possibility for atoms to have coordination numbers more than four. This corresponds to the situation of the i th and the j th atoms sharing a covalent bond.

These desired characters of the atoms can be realized by the following model potential for the interaction, which is divided into two terms, namely, the attractive one and the

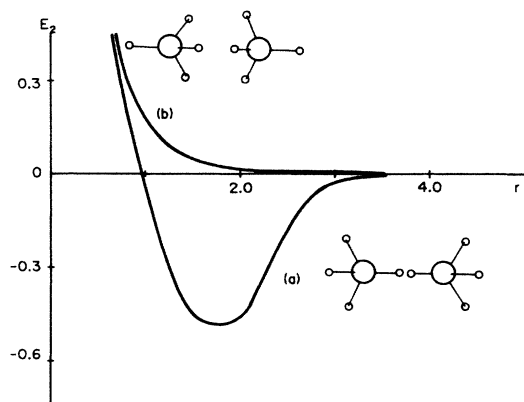


FIG. 1. Potential-energy curves of the dimer as a function of interatomic distance r when $\rho=0.8$, $a=0.7$, and $b=0.5$. The two large circles are atoms and the eight small circles are their attractive centers. Curve (a) is for the case when the attractive centers of both atoms are directed to each other, while (b) is for when they are directed opposite to the other atom.

repulsive one. The attractive part of the interaction bears the nonspherical part of the model atoms:

$$U_{\text{att}}(\mathbf{r}_{ij}; \boldsymbol{\alpha}_i, \boldsymbol{\alpha}_j) = -F_{ij}(\mathbf{r}_{ij}, \boldsymbol{\alpha}_i) F_{ji}(\mathbf{r}_{ji}, \boldsymbol{\alpha}_j), \quad (2.1)$$

where \mathbf{r}_{ij} is the position vector directed from the i th atom to the j th atom and $\boldsymbol{\alpha}_i$ are Euler's angles, representing the rotation of the attractive centers of the i th atom. The value F_{ij} depends on the distances from the j th atom to four tetrahedral attractive centers of the i th atom,

$$F_{ij}(\mathbf{r}_{ij}, \mathbf{0}) = f(|\mathbf{r}_{ij} - \mathbf{d}_{i1}|) + f(|\mathbf{r}_{ij} - \mathbf{d}_{i2}|) + f(|\mathbf{r}_{ij} - \mathbf{d}_{i3}|) + f(|\mathbf{r}_{ij} - \mathbf{d}_{i4}|), \quad (2.2)$$

where

$$f(r) = b / (r^3 + a), \quad (2.3)$$

and

$$\begin{aligned} \mathbf{d}_{i1} &= (1, 1, 1), \\ \mathbf{d}_{i2} &= (1, -1, -1), \\ \mathbf{d}_{i3} &= (-1, 1, -1), \\ \mathbf{d}_{i4} &= (-1, -1, 1). \end{aligned} \quad (2.4)$$

Vectors \mathbf{d}_{ip} 's ($p=1,2,3,4$) for $\boldsymbol{\alpha}_i=\mathbf{0}$ represent the positions of four attractive centers associated with the i th atom at the origin. These centers are rotated around the origin by angle α_i for $\boldsymbol{\alpha}_i \neq \mathbf{0}$. When the j th atom sits on one of the four attractive centers of the i th atom, the corresponding f of four f 's in (2.2), then F_{ij} takes the largest value. Hence, U_{att} , the product of F_{ij} and F_{ji} , becomes largest only when both the i th and the j th atoms sit on one of the attractive centers of the other. Therefore, the desired situation is energetically preferable in the symmetrized product form (2.1). On the other hand, when $r_{ij} \gg 1$, U_{att} is proportional to r_{ij}^{-6} , analogously to the dispersion force.

The scale of length of our model system is given by $|\mathbf{d}_{ip}| = \sqrt{3}$, which is to be interpreted as the covalent bond length, for example, 4.4. a.u. for silicon clusters, in considering the real system. It can be seen from (2.3) that the value $(b/a)^2$ gives approximately the energy gain in making a bond, while $b^{1/3}$ gives the effective range of U_{att} .

The repulsive part of the interaction mainly comes from the overlap of the core-electron clouds, and the Born-Mayer potential is often used to represent it. The Born-Mayer potential, however, is unfavorable for the structural simulation, as it remains finite when the interatomic distance close to zero. Hence, for the repulsive part of the model potential we adopt the Yukawa potential:

$$U_{\text{rep}}(r) = e^{-r/\rho} / r, \quad (2.5)$$

where r is the interatomic distance and ρ is the parameter representing the range of the repulsive potential. The numerator of $U_{\text{rep}}(r)$ has the Born-Mayer form, and the denominator makes $U_{\text{rep}}(r)$ infinite at $r \rightarrow 0$.

Finally, the total energy of the system is given as

$$E_n = \sum_{\substack{i,j=1 \\ i < j}}^n U(\mathbf{r}_{ij}; \boldsymbol{\alpha}_i, \boldsymbol{\alpha}_j), \quad (2.6)$$

where n is the number of the atoms and

$$U(\mathbf{r}_{ij}; \boldsymbol{\alpha}_i, \boldsymbol{\alpha}_j) = U_{\text{att}}(\mathbf{r}_{ij}; \boldsymbol{\alpha}_i, \boldsymbol{\alpha}_j) + U_{\text{rep}}(r_{ij}). \quad (2.7)$$

III. STRUCTURE OF THE CLUSTERS

The stable structure of our model at $T=0$ K can be found when the total energy takes the minimum value. To find it numerically, we have adopted the quasi-Newton method and calculated the stable structures of clusters for $2 \leq n \leq 20$. In the actual calculation, $n-1$ atoms are translated and rotated so as to minimize the total energy and the position and the direction of the remaining one atom are fixed throughout the calculation, corresponding to the exclusion of the translation and the rotation of the whole system.

We have examined two different sets of parameters: one set is that $\rho=0.8$, $a=0.7$, and $b=0.5$, and the other is that $\rho=0.8$, $a=0.3$, and $b=0.45$. The potential-energy curve, using the former set, is smooth from the repulsive to the attractive regions (Fig. 1), while the attractive region of the potential-energy curve with the latter parameter set becomes narrower, and the curve slightly uneven in comparison with Fig. 1(a). However, the results obtained by two different parameter sets are almost the same. The reason for this is that only the static stable structures are considered in our calculation. The dynamical properties, for example, frequencies of the lattice dynamics, melting temperature, etc., may be very sensitive to the parameter values. Here we present the results with $\rho=0.8$, $a=0.7$, and $b=0.5$.

Depending on the initial configuration, the different stable structures for the same n are found when $n \geq 5$. The calculated structures tend to have four-, five-, and six-membered rings. The clusters with only six-membered rings are found for $n=6, 7, 8, 10, 11, 14, 15, 18$, and 19,

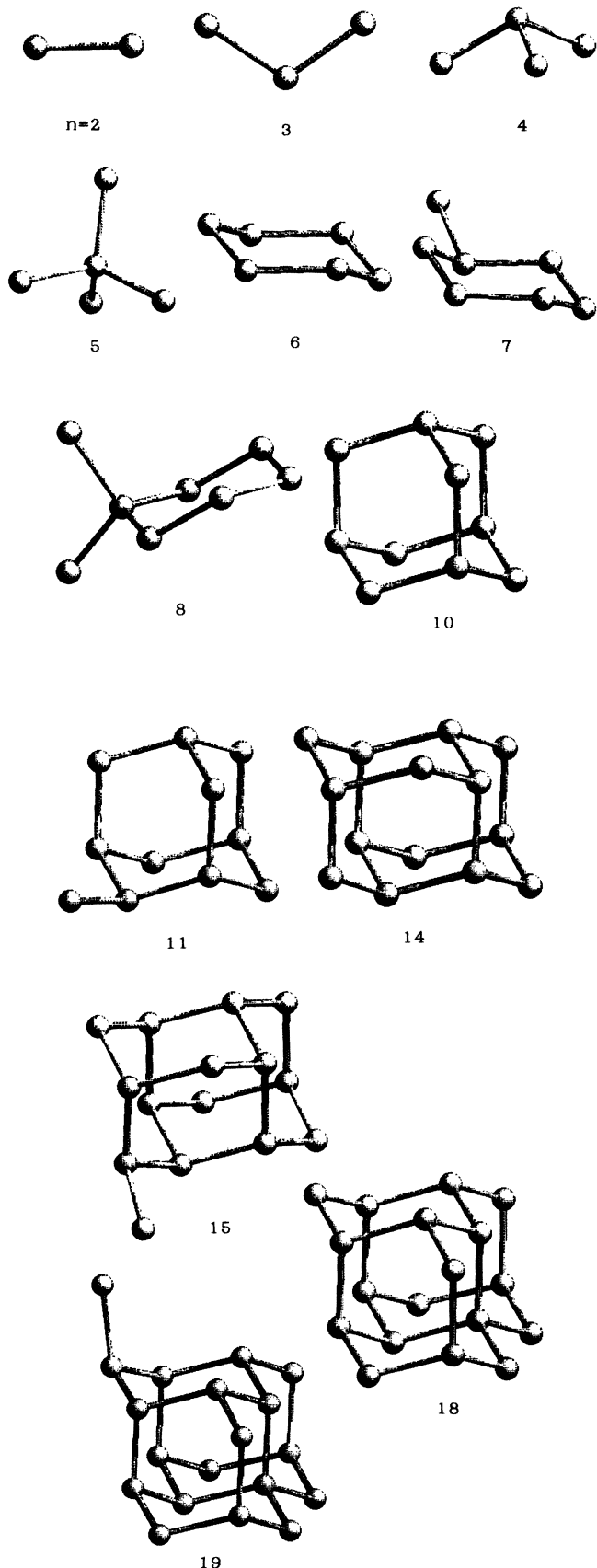


FIG. 2. Calculated structures of the clusters by the use of the model potential. For $n \geq 6$, the clusters with only six-membered rings are shown.

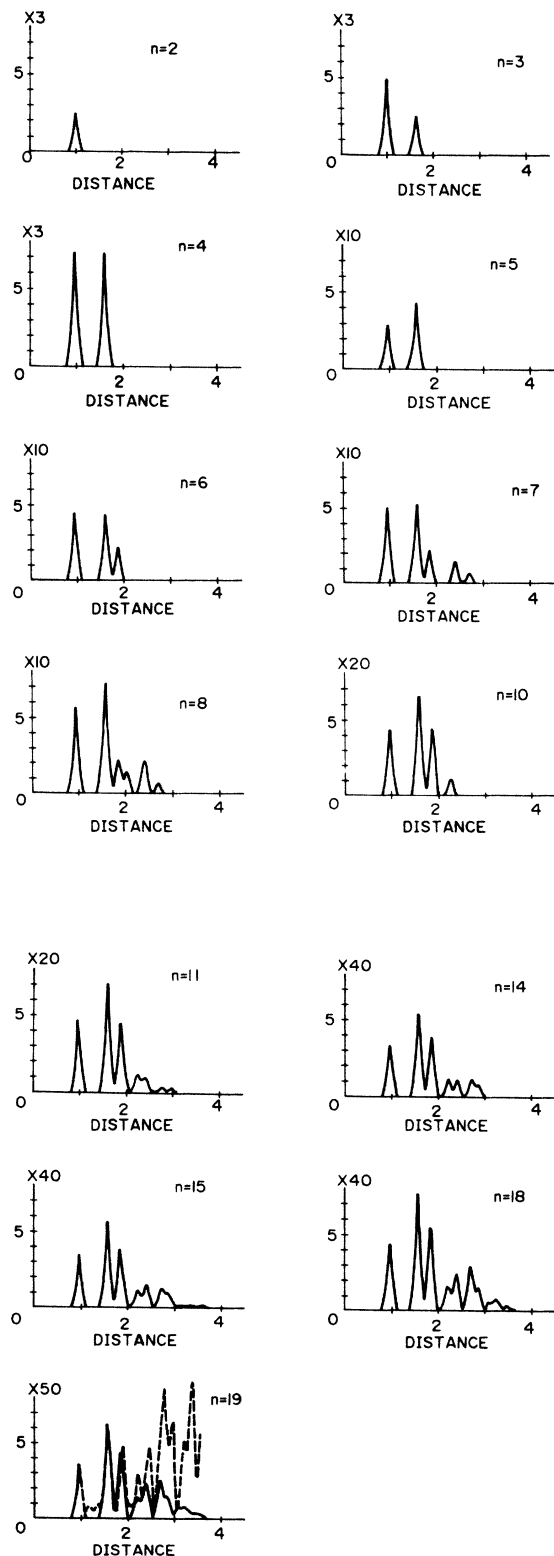


FIG. 3. Pair distribution functions (PDF's) of the clusters in Fig. 2. δ functions are replaced by the Gaussian distribution functions with the variance 0.003. The distance is normalized so that the peak of $n=2$ is at 1.0. The experimental radial distribution function of crystalline germanium (Ref. 7) is shown (dashed line) together with the PDF of $n=19$ in arbitrary units.

and have structures similar to partial frameworks of the diamond lattice. Including the clusters of $n = 2, 3, 4,$ and 5 , the structures of this series are shown in Fig. 2. The pair distribution functions (PDF's) of this series coincide well with the radial distribution function (RDF) of the diamond lattice (Fig. 3). PDF of the $n = 19$ cluster in Fig. 2 has peaks at exactly the same positions as those of the experimental RDF peaks of crystalline germanium.⁷ So, we call this series the "crystalline series." The total energy of this series is plotted against the number of the bonds in Fig. 4. The total energy is almost proportional to the number of the bonds. Hence, our tetrahedral potential model is consistent with the bond-energy concept, which is known to be applicable to the covalent bonds to the first approximation.

The other series, clusters with mainly four- and five-membered rings, have the structures resembling partial frameworks of the stable structure of the cluster with 20 atoms, which is a regular dodecahedron (Fig. 5). When $n < 20$, the lack of one atom from five-membered rings gives rise to four-membered rings. PDF's of the clusters of Fig. 5 are shown in Fig. 6. On the other hand, the RDF of amorphous Ge has the peaks at 1.0, 1.6, and 2.45 (shown together with the PDF of $n = 20$ at Fig. 6). The characteristic feature of the RDF's of amorphous Si and Ge is the absence of the third peak of the crystalline phase (the peak at 1.9). As the PDF of a dodecahedron ($n = 20$) clearly shows, PDF's in Fig. 6 also lack this peak. So, we call these clusters the "amorphous series." The bond angle of the regular dodecahedron is 108° , which is nearly the same value as the crystalline one, i.e., 109° . We have found that the energy loss of the distortion to make five-membered rings is very small if we use our parameter values for ρ , a , and b . On the other hand, the number of the rings of the amorphous series is the same or more than that of the crystalline series of the same size n . This makes the total energy of the amorphous series lower than that of the crystalline series.

In the amorphous series, the competition between the

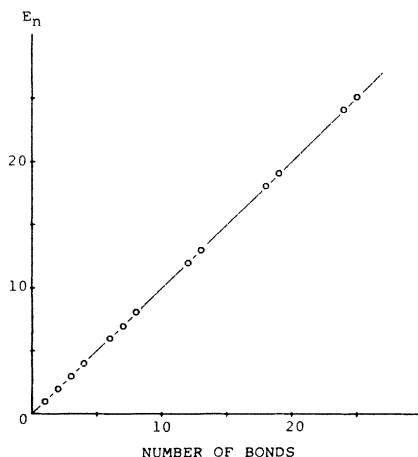


FIG. 4. Absolute values of the total energy vs the number of bonds. Plotted values are the total energies divided by E_2 , which is -0.542 .

energy loss by the distortion and the energy gain due to the increase of the number of the rings depends upon the values of the potential parameters. We have investigated such a competition and found that the crystalline series is more stable when b is very small, for example, $b = 10^{-4}$, while $b/a = 1$. This comes from the fact that the parameter b determines the range of the attractive part and the energy loss of the distortion of the bond angle from 109° to 108° is large for the potential with a sharp minimum.

IV. MAGIC NUMBERS

The cluster sizes, n , corresponding to the peaks of time-of-flight mass spectra, are called magic numbers. The corresponding clusters are thought to have relatively large binding energy per atom. To find the magic numbers of our model, we plot the binding energy per atom

$$\epsilon_n = |E_n| / n, \quad (4.1)$$

against n for both crystalline and amorphous series in Fig. 7.

In the amorphous series, the value of ϵ_5 is almost the same as that of ϵ_6 but greater than ϵ_4 . Also, ϵ_{10} , ϵ_{12} , ϵ_{16} , ϵ_{18} , and ϵ_{20} are local peaks. Hence, the magic numbers of this series are 5, 10, 12, 16, 18, and 20. In the same way, those of crystalline series are found to be 6, 10, 14, and 18.

V. DISCUSSION

The calculated stable structures have a tendency to form connected rings. As mentioned before, our tetrahedral model potential is based on the bond-energy concept. Therefore, the cyclic structure having an additional bond, as compared with the chain structure, turns out to be more stable.

The correspondence between the PDF of a regular dodecahedron and the RDF of an amorphous Ge is noteworthy. When the structure of the amorphous Ge (or Si) is considered as that obtained by rearranging the pair bonds of the diamond structure,⁸ seven-membered rings, as well as five-membered rings, are expected to appear. However, our results suggest that the five-membered ring is the main local structure of the amorphous Ge, and especially of the hydrogenated amorphous Ge. It can be seen from the plot of ϵ_n in Fig. 7 that the structures with five-membered rings are more stable than those with six-membered rings, although the former cannot form long-range order. Hence, the amorphous Ge, which has only short-range order, is likely to include the five-membered rings.

According to the appearance of two series of stable structures, the amorphous and the crystalline series, the magic numbers of our model are obtained for each series. In the amorphous series as shown in Fig. 5, the number 5 corresponds to a regular pentagon, while 10 and 20 correspond to half of and the whole of a regular dodecahedron, respectively. The structure of $n = 12$ has four loops as

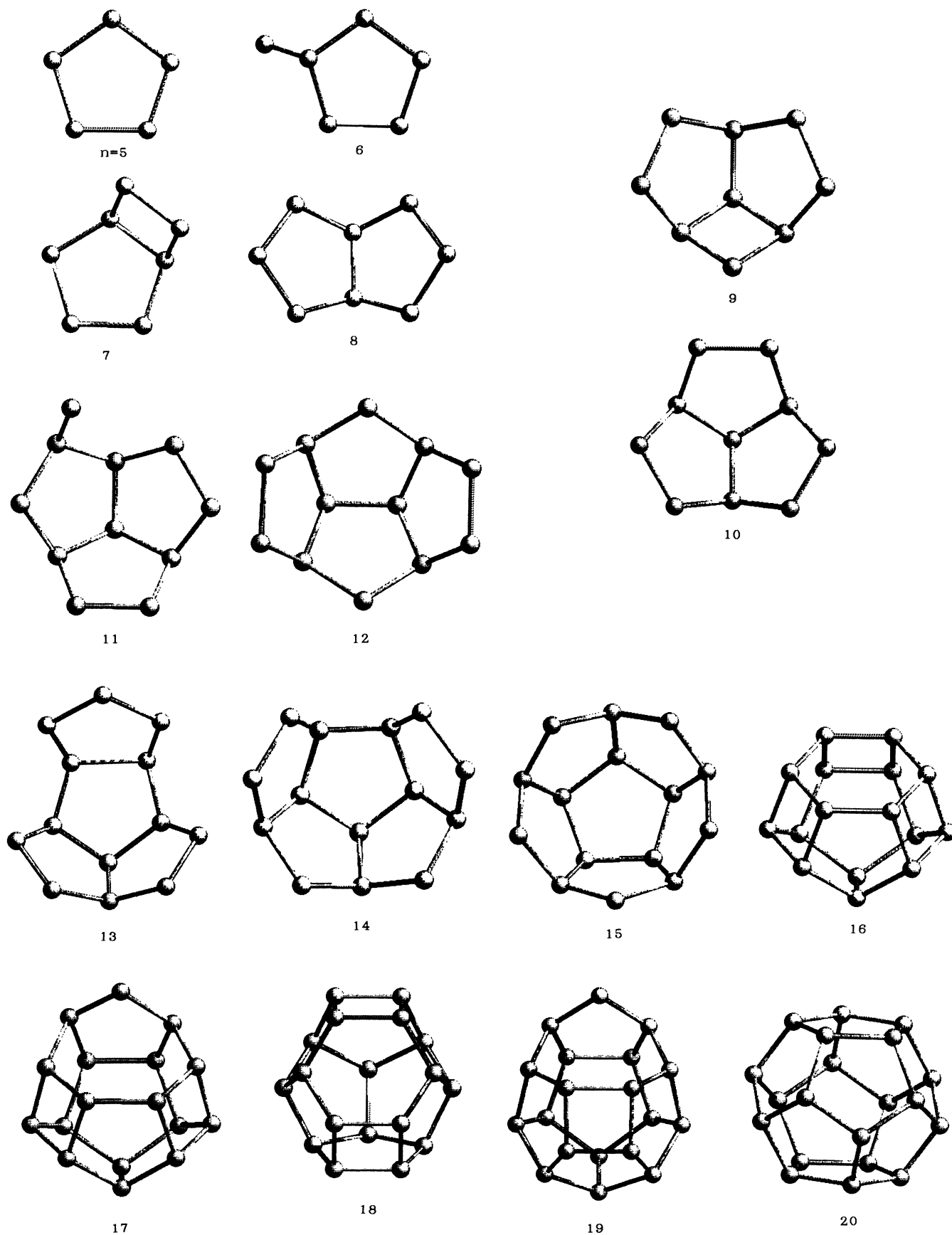


FIG. 5. Calculated structures of the clusters consisting of mainly five-membered rings.

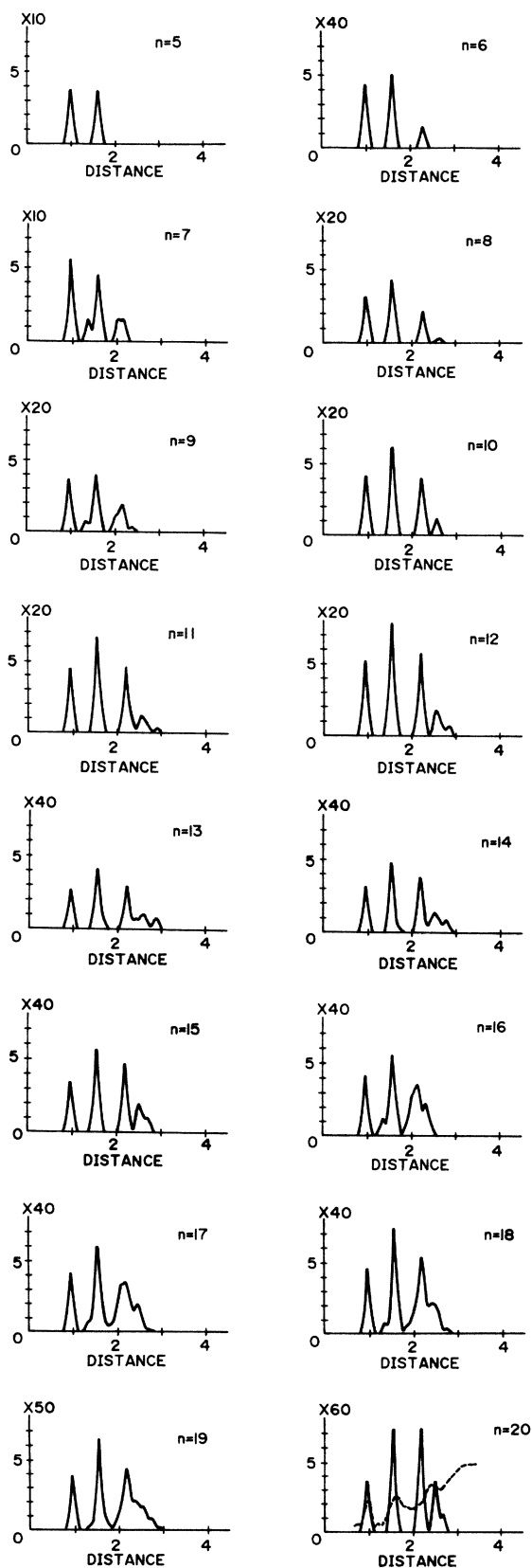


FIG. 6. Pair distribution functions of the clusters in Fig. 5. The variance of the Gaussian distribution function is again 0.003. Experimental radial distribution functions of amorphous germanium (Ref. 7) are shown by a dashed line on the figure for $n = 20$ (arbitrary units).

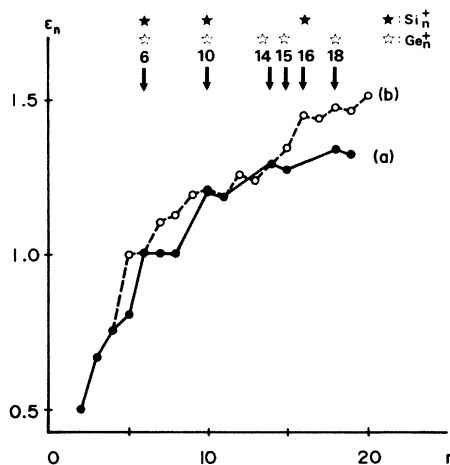


FIG. 7. Calculated binding energy per atom against the number of the atoms for (a) the crystalline series and (b) the amorphous series. The values are given in units of $|E_2|$. Numbers marked with arrows are the observed magic numbers of Si_n^+ (Ref. 4) and Ge_n^+ clusters (Ref. 5).

does that of $n = 13$. The other peaks, 16 and 18, come from the mixing of four-membered rings. In the crystalline series, the magic numbers are 6, 10, 14, and 18, which have period 4. When the pyramidal cluster consisting of four atoms sits on an equilateral triangle of the atoms of the (111) surface of diamond structure, as seen in the formation of $n = 10$ (adamantene structure) from $n = 6$ (cyclohexane structure) of Fig. 2, the number of rings increases by three and, the number of bonds by six. The period of magic numbers, 4, comes from this large increase in the number of bonds. It is interesting to note that the pyramidal cluster of four atoms is the same as that found in the reconstruction model of the $\text{Si}(111)7 \times 7$ surface.^{9,10}

In our model calculation, we have used the potential-parameter values which are not specified for any element of group IV. Our results on the structure and the magic numbers would be applicable to any sp^3 microclusters as far as the bond-energy concept is valid. One experiment on C_n^+ clusters¹¹ has shown that the magic numbers are 3, 5, 7, 10, 14, 18, and 22, and another experiment,³ 3, 11, 15, 19, and 23. Our result of the crystalline series is closer to the former. The period of 4 of our magic numbers is found in both experiments. Some disagreements might be attributed to a deviation from the sp^3 bond.

The experiment on Si_n^+ clusters has also been done⁴ and the magic numbers obtained are 6, 10, and 16, which are also close to those of our crystalline series. The magic numbers of Ge_n^+ have been found⁵ to be 6, 10, 14, 15, 18, and 22. This also supports the crystalline series of our model. The difference between C and Si (Ge) clusters may come from the sp^2 σ -bond and the π -bond properties of C atoms as found in graphite. It is reasonable that the calculation by the use of our model potential better simulates the properties of Si and Ge clusters.

The magic numbers of the amorphous series, 10 and 16, are also observed in Si_n^+ clusters. However, the important peaks of 5 and 20 are missing in the experiment. The

absence of the amorphous series in the experiment might be due to the experimental condition for creating the initial clusters. It would be interesting to examine the change of the magic numbers by changing the conditions for creating initial clusters, for example, by using amorphous silicon.

The dangling bonds of the $n=5$ cluster of the amorphous series are directed outward from the cluster and will have weak interaction between them. On the other hand, the $n=6$ cluster of the crystalline series has two sets of three dangling bonds parallel to each other, i.e., the dangling bonds of the (111) surface of the diamond structure. These dangling bonds will interact with each other strongly and the equilateral triangle of the (111)-surface atoms contracts to attain a larger π -bond stabilization.¹² Then, the cluster can achieve relatively large energy gain by the reconstruction. This reconstruction mechanism might make the crystalline series more stable, as shown experimentally.

Our tetrahedral model potential, taking into account

the main characteristics of the sp^3 bonds, is very powerful in presuming the stable structures and the total energies of microclusters because of its simplicity. However, the model takes no account of a deviation from the sp^3 bond which may be caused by the interaction between the dangling bonds. Such a deviation has been shown to play an important role in giving the actual structure of Si microclusters.¹² Even in this case, the structure can be understood as a reconstructed form of the initial sp^3 structure, which can be calculated by using the model potential presented in this paper.

ACKNOWLEDGMENTS

The authors would like to thank Dr. C. Satoko (Institute for Molecular Science, Okazaki), Dr. Y. Ishii (Institute for Solid State Physics, Tokyo), and Dr. A. Oshiyama (NEC Corporation, Kawasaki) for their useful discussions.

¹I. A. Harris, R. S. Kidwell, and J. A. Northby, *Phys. Rev. Lett.* **53**, 2390 (1984).

²W. D. Knight, K. Clemenger, W. A. de Heer, W. A. Saunders, M. Y. Chou, and M. L. Cohen, *Phys. Rev. Lett.* **52**, 2141 (1984).

³E. A. Rohlfing, D. M. Cox, and A. Kadlor, *J. Chem. Phys.* **81**, 3322 (1984).

⁴L. A. Bloomfield, R. R. Freeman, and W. L. Brown, *Phys. Rev. Lett.* **54**, 2246 (1985).

⁵T. P. Martin and H. Schaber, *J. Chem. Phys.* **83**, 855 (1985).

⁶M. R. Hoare, *Adv. Chem. Phys.* **40**, 49 (1979).

⁷R. J. Temkin, W. Paul, and G. A. N. Connel, *Adv. Phys.* **22**, 581 (1973).

⁸F. Wooten, K. Winer, and D. Weaire, *Phys. Rev. Lett.* **54**, 1392 (1985).

⁹M. Aono, R. Souda, C. Oshima, and Y. Ishizawa, *Phys. Rev. Lett.* **51**, 801 (1983).

¹⁰M. Tsukada and C. Satoko, *Surf. Sci.* **161**, 289 (1985).

¹¹J. Friedel, *Helv. Phys. Acta* **56**, 507 (1983).

¹²S. Saito, S. Ohnishi, C. Satoko, and S. Sugano (unpublished).

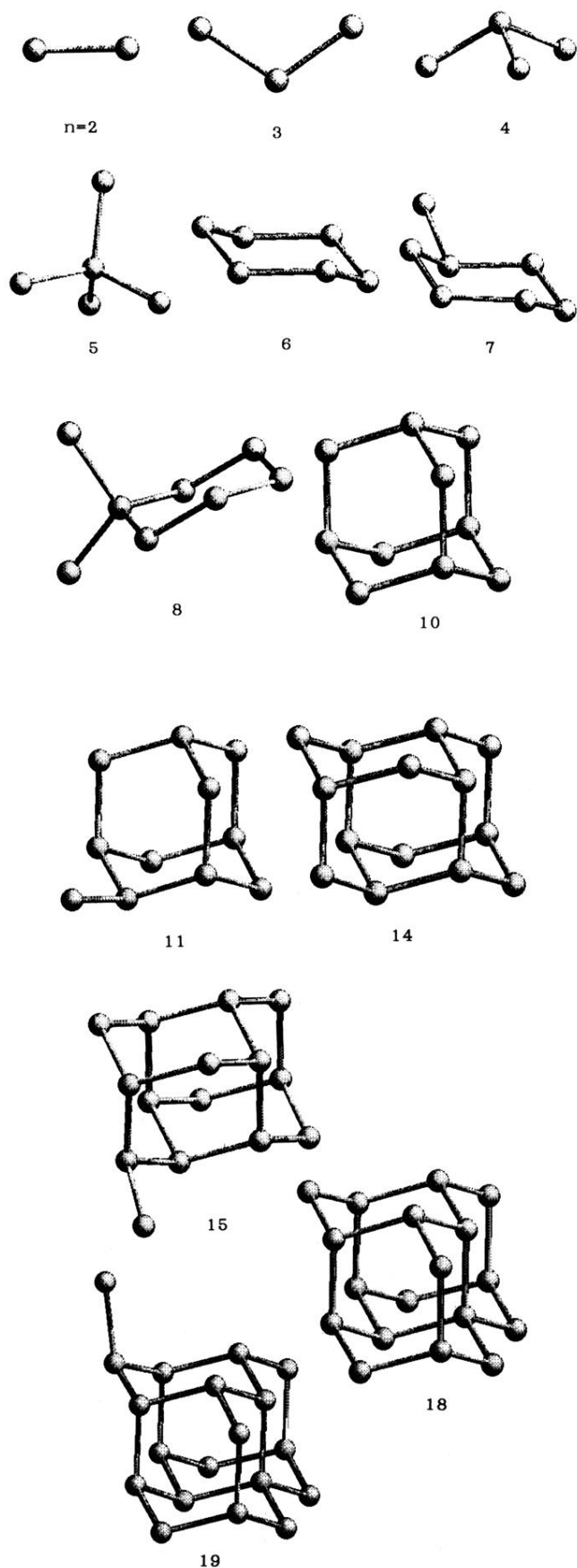


FIG. 2. Calculated structures of the clusters by the use of the model potential. For $n \geq 6$, the clusters with only six-membered rings are shown.

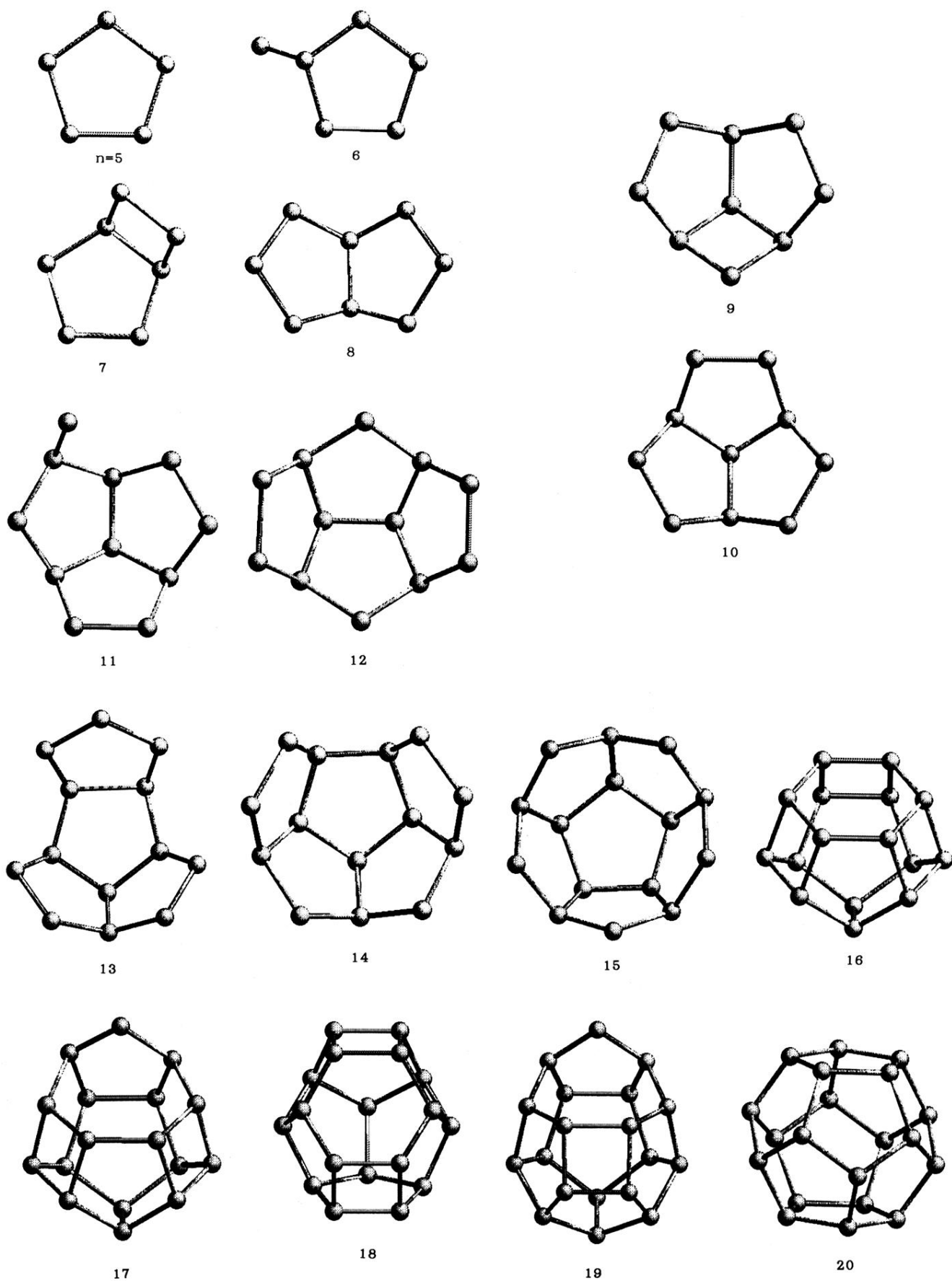


FIG. 5. Calculated structures of the clusters consisting of mainly five-membered rings.